HHS Public Access

Author manuscript

Circ Arrhythm Electrophysiol. Author manuscript; available in PMC 2020 June 05.

Published in final edited form as:

Circ Arrhythm Electrophysiol. 2019 June ; 12(6): e006942. doi:10.1161/CIRCEP.118.006942.

Cardiac Afferent Denervation Abolishes Ganglionated Plexi and Sympathetic Responses To Apnea: Implications For Atrial Fibrillation

Liliana Tavares, MD[1], **Moisés Rodríguez-Mañero, MD, PhD**[2], **Bahij Kreidieh, MD**[1], **Sergio H. Ibarra-Cortez, MD**[1], **Jiexiao Chen, BS**[1], **Sufen Wang, PhD**[1], **Judit Markovits, DVM, PhD**[3], **Roberto Barrios, MD**[4], and **Miguel Valderrábano, MD**[1]

[1]Dept of Cardiology, Houston Methodist DeBakey Heart & Vascular Center, Houston Methodist Hospital, Houston Methodist Research Institute, Houston, TX

[2]Cardiology Department, Hospital Universitario Santiago de Compostela. Santiago de Compostela. IDIS. Spain. Centro de Investigación Biomédica en Red de Enfermedades Cardiovasculares (CIBERCV CB16/11/00226 - CB16/11/00420)

[3]Dept of Pathology, Comparative Medicine Program, Houston Methodist Research Institute, Houston, TX

[4]Dept of Pathology, Houston Methodist Hospital, Houston Methodist Research Institute, Houston, TX;

Abstract

Background: The autonomic nervous system response to apnea and its mechanistic connection to atrial fibrillation (AF) are unclear. We hypothesize that sensory neurons within the ganglionated plexi (GP) play a role. We aimed to delineate the autonomic response to apnea and to test the effects of ablation of cardiac sensory neurons with resiniferatoxin (RTX), a neurotoxic transient receptor potential vanilloid 1 (TRPV1) agonist.

Methods: Sixteen dogs were anesthetized and ventilated. Apnea was induced stopping ventilation until oxygen saturations decreased to 80%. Nerve recordings from bilateral vagal nerves, left stellate ganglion (SG) and anterior right GP (ARGP) were obtained before and during apnea, before and after RTX injection in the ARGP (Protocol 1, n=7). Atrial effective refractory period (ERP) and AF inducibility upon single extrastimulation were assessed before and during apnea, and before and after intrapericardial RTX administration (Protocol 2, n=9). GPs underwent immunohistochemical staining for TRPV1.

Results: Apnea increased ARGP activity, followed by clustered crescendo vagal bursts synchronized with heart rate and blood pressure (BP) oscillations. Upon further oxygen desaturation, a tonic increase in SG activity and BP ensued. Apnea induced ERP shortening from 110.20±31.3 ms to 90.6±29.1 ms ($p<0.001$), and AF induction in 9/9 dogs vs 0/9 at baseline. After

Correspondence: Miguel Valderrábano, MD, Director, Division of Cardiac Electrophysiology, Department of Cardiology, Houston Methodist Hospital, 6550 Fannin St, Suite 1901, Houston, TX 77030, Tel +1 713 441 5231, Fax 713 793 7032, mvalderrabano@houstonmethodist.org.

Disclosures: None

RTX administration, increases in GP and SG activity and BP during apnea were abolished, ERP *increased* to 126.7±26.9 ms (p=0.0001), and AF was not induced. Vagal bursts remained unchanged. GP cells showed cytoplasmic microvacuolization and apoptosis.

Conclusions: Apnea increases GP activity, followed by vagal bursts and tonic SG firing. RTX decreases sympathetic and GP nerve activity, abolishes apnea's electrophysiological response and AF inducibility. Sensory neurons play a role in apnea-induced AF.

Journal Subject Terms

Atrial Fibrillation; Animal Models of Human Disease; Autonomic Nervous System

Keywords

autonomic nervous system; obstructive sleep apnea; atrial fibrillation; cardiac ganglionated plexi; sensory neurons

Introduction

Obstructive sleep apnea (OSA) is associated with atrial fibrillation (AF). The precise mechanisms of apnea-induced susceptibility to AF are unclear. Numerous possible mechanisms responsible for this association have been proposed including autonomic dysfunction.

Apnea induces a response of the cardiac autonomic nervous system (ANS) that may increase AF vulnerability.[1–3] The cardiac ANS comprises the extrinsic cardiac autonomic system, centrally derived parasympathetic and sympathetic nerves, and the intrinsic cardiac autonomic system, which consists of epicardial ganglionated plexi (GP) embedded in fat pads that contain efferent parasympathetic and sympathetic neurons, interneurons, afferent sensory neurons and others.[4, 5] The integrated response of the ANS to apnea and its role in AF susceptibility have not been delineated. Of particular interest is that GP sensory neurons are thought to mediate a local neurosensory reflex in response to mechanical or chemical stimuli, such as acidosis, hypoxia, and hypercarbia, mediated by substance P (SP),[6, 7] calcitonin gene-related peptide (CGRP)[6] and others. We hypothesized apnea could be a potent stimulator of sensory neurons.

Resiniferatoxin (RTX) (Figure 1A), an ultra-potent analogue of capsaicin, the active compound of chili peppers,[8, 9] causes the transient receptor potential vanilloid 1 (TRPV1), present in sensory neurons, to become permanently permeable to cations,[10] particularly the calcium cation, leading to a powerful stimulation effect followed by neuronal death, desensitization and analgesia.[11–13] RTX has been shown to reduce sympathetic activation and cardiac remodelling in heart failure.[14]

We sought to delineate the autonomic response to apnea, its hemodynamic and electrophysiological correlates, and to test the effects of chemical ablation of cardiac GP sensory neurons with RTX.

Methods

The data that support the findings of this study are available from the corresponding author upon reasonable request.

The animal protocol used was approved by the Institutional Animal Care and Use Committee of the Houston Methodist Hospital. A detailed description of the methods is available in the online supplement. A total of sixteen mongrel dogs, were intubated and ventilated (Harvard Apparatus Co., Natick, MA) under general anesthesia. Apnea was induced by disconnecting the ventilator tube at end expiration until oxygen saturation (SaO_2) dropped at least to 80%.

Protocol 1

Under continuous electrocardiographic and hemodynamic monitoring, after median cervical incision and sternotomy, the anesthesia agent was switched to alpha chloralose. Bilateral vagal, left stellate ganglion (SG), and anterior right GP nerve recordings were obtained (n=7) before and during apnea episodes, before and after local RTX injection in the anterior right GP (Figure 1B, C, D and E).

Epicardial fat pads known to contain the anterior right, right and left inferior and left superior GPs were sampled and the following histological studies were performed: hematoxylin and eosin (H&E) staining and TRPV1 and CGRP immunohistochemical staining. Terminal deoxynucleotidyl transferase dUTP-mediated nick end labeling (TUNEL) assay was also performed to detect apoptotic cells.

Protocol 2

Left atrium (LA) geometry maps were performed after a trans-septal puncture using NavX guidance. A subxiphoid pericardial puncture was performed and a sheath inserted in the oblique sinus. Effective refractory period (ERP) measurements were measured in 3 sites in the LA before and during apnea, before and after intrapericardial RTX injection (Figure 1F, G, H and I).

Figure 1 shows a schematic representation of both protocols.

Results

Protocol 1

Autonomic response to apnea

Anterior right GP activity.: At apnea initiation, sparse bursts of GP activity were noted which appeared to subside shortly thereafter. As apnea progressed and SaO_2 declined, a consistent increase in GP activity was seen. Figure 2A illustrates GP activity at baseline and during apnea, noted to be most intense at 2 min of apnea.

Vagal activity.: Immediately upon initiation of apnea, no detectable changes were present in the vagal recordings. However, as SaO_2 declined, crescendo phasic bursts of vagal discharges appeared, which coincided with heart rate (HR) and blood pressure (BP)

oscillations. The onset of detectable bursts occurred after 104.97±44.33 seconds into apnea, when SaO_2 was 91.85±6.12%. Each burst coincided with HR and BP changes. Figure 3 shows an example, including vagal activity quantification divided by tertiles. The progressive increase in vagal bursts during apnea was significant (from burst onset to apnea end, all tertiles $p< 0.001$, significance level set at $p<0.017$). The number of spikes per burst, the duration and density of bursts (spikes per burst duration) increased, and the interburst delay (time between bursts) decreased significantly in the final tertile towards the end of apnea. Of note, the phasic bursts coincided in all cases with the *upsloping* phase of HR and the *downsloping phase* of BP oscillations, whose frequency matched the burst frequency. The phasic relationship between vagal bursts and HR-BP oscillations was consistent in all animals.

Sympathetic activity.: Upon apnea initiation, a decrease in stellate ganglion (SG) amplitude was seen, but as apnea continued and SaO_2 declined, there was a progressive increase in SG recording amplitude that coincided with HR and BP increases ("BP rebound", Figure 4A). The increase in SG activity, contrary to vagal firings, had a tonic pattern rather than phasic bursts. The SG amplitude began to increase as SaO_2 declined to an average of 93.24 ±5.15 %, and persisted beyond resumption of breathing for 65.67 ±38.84 seconds, closely matching the rebound HR and BP. Subcutaneous (SC) nerve activity as an estimate of the sympathetic tone[15] closely matched that of the SG, as recorded in 3 dogs. Figure 4B shows SG and SC responses to apnea.

Vagal, SG, and GP nerve activity recovered back to baseline values once apnea was terminated.

Acute GP-RTX-induced changes—Anterior right GP (ARGP) RTX injection led to dramatic increases in BP within less than 20 minutes of infusion in all animals, which more than doubled. HR also increased but less dramatically. Figure 5A illustrates an example of immediate RTX-induced changes caused by local RTX injection. The increases in BP were paralleled by increases in ARGP activity (Figure 5B). Eventually, hemodynamic changes subsided. Time from RTX administration to re-normalization of BP and HR ranged from 15 to 40 min.

Autonomic response to apnea after RTX administration—Following recovery from acute RTX effects, the baseline hemodynamics in eupneic state were regained. In contrast to baseline recordings, GP and SG recordings during apnea after RTX activity showed no detectable increased activity during apnea (Figures 2B and 4C). Additionally, the BP rebound increase upon late desaturation was blunted (Figure 4C and Supplemental Figures 1 and 2).

Vagal nerve activity, however, did not change, with preserved phasic bursts during desaturation and preserved phasic relationship between vagal bursts and HR and BP (Supplemental Figure 3). The unaltered vagal response was also shown by the fact that bradycardic responses to cervical vagal stimulation were unaffected by RTX administration (HR decreases of 35 ±13 bpm vs 34 ±12 bpm, respectively; p=0.5) (Supplemental Figure 4).

Histopathology studies—All epicardial fat pads sampled contained ganglion cells (Figure 6A) with positive staining for sensory neuronal markers TRPV-1 and CGRP. Non RTX injected GPs (control, saline injected) were positive for TRPV1 and CGRP and cells were not apoptotic (TUNEL-negative) (Figure 6A). RTX injected GPs showed individual ganglion cells with cytoplasmic micro and macro vacuolization, had blunted staining for TRPV1 and CGRP, and cells were apoptotic (TUNEL-positive) (Figure 6B).

Protocol 2.

Electrophysiological response to apnea before RTX administration—Atrial ERP (AERP) decreased during apnea from 110.20 ±31.3 ms to 90.6 ±29.1 ms, ($p<0.001$, significance level set at $p<0.025$).

AF could only be induced once (4.2%) from a total of 24 eupneic-state atrial single extrastimulations. Conversely, during apnea, AF was induced at least once in every single dog. In 24 apneic episodes, AF was successfully induced 14 times (58.3%; mean duration = 2.23 ±2.9 minutes, requiring successful cardioversion in 3 episodes (Figure 7).

Electrophysiological response to apnea after RTX administration—Acute hemodynamic and electrocardiographic changes occurred after intrapericardial RTX (Figure 5C and D) and fully recovered in 7/9 dogs. These were similar to those observed in Protocol 1.

Post-RTX apnea induced significant *increases* in AERP from 107.6±23.9 to 126.7 ±26.9 ms ($p<0.001$). The eupneic AERP was unchanged from baseline (110.2±31.3 vs 107.6±23.9, $p=0.9$), which suggests a lack of RTX-induced changes in eupneic myocardial refractoriness.

After RTX, AF could only be induced once (4.2%) from a total of 21 eupneic state atrial single extrastimulations and could no longer be induced during apnea in any of the 21 apneic induction attempts performed.

Discussion

Our studies show several novel findings. First, we delineate the integrated autonomic response to apnea, which includes a consistent sequence of events upon oxygen desaturation (graphic abstract), including: 1) Increases in GP activity; 2) Progressively increasing phasic bursts of vagal activity, which closely correlate with HR and BP oscillations; and 3) Tonic increase in sympathetic activity, which correlates with steady increases in HR and SBP. Second, we correlate these autonomic changes with electrophysiological changes, namely ERP shortening and consistent AF induction with single extrastimulation during apnea. Third, we show the acute effects of RTX administration, both locally as well as intrapericardially, which are characterized by a dramatic increase in anterior right GP (ARGP) activity and BP, and increases in HR. Such sympathetic afferent activation, along with its associated hemodynamic effects, can lead to additional electrophysiological changes, including spontaneous VF, but is characteristically transient, and followed by recovery to a baseline physiological state. Fourth, we show that apnea post-RTX lacked ARGP activation, and lacked the increased SG and rebound BP associated with

deoxygenation. Additionally, RTX eliminated both apnea-induced AERP shortening and AF inducibility; and after RTX treatment, apnea led to prolonged AERP.

These results are consistent with a fundamental role of the cardiac autonomic nervous system mediating the electrophysiological responses of the atrial myocardium to apnea and suggest the cardiac afferents as a possible therapeutic target for autonomic modulation.

ANS response to apnea: hemodynamic and electrophysiological correlates

The consistent sequence of events we detected seems to initiate with slow, steady decreases in HR followed by HR and BP oscillations and later by a BP rebound increase (graphic abstract). An initial increase in GP activity subsided to then increase, particularly at the end of apnea. The onset of HR oscillations preceded the onset of phasic bursts of vagal discharges, whose frequency, amplitude and spike density grew as apnea persisted. The crescendo nature of these bursts was paralleled by an increase in the frequency of HR and BP oscillations, which supports a mechanistic connection. Of note, vagal bursts coincided with the upsloping phase of HR oscillations and the downsloping phase of BP oscillations. The mechanistic origin of such vagal bursts is unclear, but could represent afferent activity since most fibers in the vagal nerves are afferent,[16, 17] or originate from sympathetic efferents of the vagus leading to HR increases,[18] or be parasympathetic efferents with either primary effects on BP or delayed effects on HR.

Coinciding with the onset of oxygen desaturation, a tonic increase in sympathetic (SG) activity was found, which matched the onset of a steady increase in BP. Subcutaneous nerve activity matched the SG activity, as previously reported.[15] The GP and SG activity and the BP rebound were abolished by RTX injection.

Role of the ANS and sensory neurons in the genesis of AF in apnea

Previous experimental studies have demonstrated a close mechanistic association between the cardiac ANS and apnea-induced AF, focusing mainly on parasympathetic contributors.[2, 19] In a canine model of apnea, Ghias et al documented increases in neural activity within the GP prior to the initiation of AF.[1] Furthermore, ablation of the Ao-SVC ganglionated plexus significantly diminished the inducibility of AF. We expand their findings to show the orchestrated intrinsic (GP) vs extrinsic ANS (vagal and SG) response to apnea and their changes after RTX.

Sensory neurons are an integral part of the GP. GP local sensory neurons are thought to mediate a local neurosensory reflex within the GP.[20] The overall physiological effect of sensory neurons activation is a depolarization of postganglionic parasympathetic neurons,[21, 22] thus enhancing GP output and leading to the local release of acetylcholine and the electrophysiological effects that follow (namely ERP shortening). This effect could be occurring at a local GP level. The mechanical and chemical stimuli to which sensory neurons react under physiological conditions is unclear, but it makes physiological sense to hypothesize that apnea-induced hypoxia, hypercarbia, acidosis, or mechanical stretch may play a role. Our data supports such contention.

We propose a reflex model of apnea-induced AF susceptibility. Apnea directly causes hypoxia, hypercarbia and acidosis. Either by chemoreceptors sensing pH, pO_2 or pCO_2, or mechanoreceptors sensing increased pressure, sensory neurons would be activated via TRPV1. Sensory neurons have the somata in the dorsal root ganglia, in the nodose ganglion of the vagus, and in the intrinsic cardiac nervous system (ICNS) themselves.[20] Local ICNS sensory neuron activation could activate postganglionic parasympathetic neurons,[21, 22] thus forming a local reflex arc that leads to ERP shortening in neighbouring myocardium. Sympathetic afferents enter through the stellate ganglia and the spinal cord and terminate in the nucleus of the solitary tract,[23] leading to increased sympathetic outflow. Both the local effect leading to ERP shortening and AF inducibility as well as the increased sympathetic outflow are abolished by RTX-induced sensory neuron ablation. Vagal responses were unchanged. The lack of vagal effects suggests that either parasympathetic afferents were not affected, or perhaps more likely, that they are mediated by non-GP afferents, either pulmonary or carotid.

After RTX, apnea induced *prolongation* of the ERP rather than shortening. This is consistent with direct myocardial effects of hypoxia, hypercarbia or acidosis, increasing post-repolarization refractoriness, analogous to the myocardial effects of ischemia,[24] which are normally counteracted by the neuronal reflexes described.

Acute RTX effects

Sensory afferents mediate the cardiac sympathetic afferent reflex, thought to lead to sympathoexcitation in heart failure and acute ischemia[13] RTX applied to the epicardium in rats can abolish this response,[13, 14] and leads to loss of TRPV1-expressing neurons, which in turn has been associated with reduced fibrosis in ischemia-induced heart failure.[14] The acute hemodynamic effects of RTX *in vivo* have been described.[25] Consistent with transient hyperactivation of cardiac sympathetic afferents, RTX led to marked GP activity, doubling of the SBP, increases in HR, and significant electrocardiographic changes (ST elevation, T-wave inversion, and even VF). These changes completely subsided and normalized over the course of up to 40 minutes, consistent with the time course from RTX-induced activation followed by neuronal toxicity.

Clinical implications

Sleep apnea is associated with AF. Multiple mechanisms are involved, but a prominent role of the autonomic nervous system is suspected. Here we delineate the integrated autonomic response to apnea, that includes GP, vagal, and SG firings in a consistent manner that leads to hemodynamic and electrophysiological (shortened ERP) changes that culminate in AF inducibility. The GP and SG responses were abolished by sensory neuron ablation with RTX. Sensory neurons mediate the electrophysiological response to apnea and could be a valid therapeutic target to reduce apena-induced AF.

Study limitations

OSA-induced AF is multifactorial and is likely to involve a plethora of mechanisms that were not studied here as hypertension, obesity, metabolic syndrome, atrial structural remodelling, among others.[26] The animal model used in this study is merely an acute model,

and not an exact replica of OSA as it does not reproduce all events associated with long-term OSA. However, this approach reproduces the hypoxia, hypercarbia, and acidosis of OSA as putative triggers of an autonomic response in an acute model of apnea and eliminates other confounding factors such as obesity, metabolic syndrome, and intrathoracic pressure dynamics that can confound a mechanistic response of the sensory neurons.

Future studies are needed to investigate the chronic effects of chemical ablation of cardiac GP sensory neurons. Chronically repeated OSA episodes has been shown to cause cardiac remodeling with fibrosis playing a prominent role which contributes to AF promotion.[27]

We did not record signals from all GPs as we were limited by anatomical access to the ARGP. Additionally, peripheral blood CO_2 and pH were not monitored. Although the mechanistic implications are significant, basic electrophysiologic properties, such as action potential duration, and conduction velocity, were beyond the scope of this study. There could be concerns about the specificity of RTX effects. However, it should be highlighted that prior studies have consistently shown the absence of myocardial effects.[8, 10, 13]

Conclusions

Apnea leads to a complex response of the cardiac autonomic nervous system including GP firing, phasic vagal bursts coinciding with HR and BP oscillations, and tonic SG firing that lead to ERP shortening and increased in AF vulnerability. Chemical ablation of intrinsic cardiac sensory neurons with RTX decreases sympathetic and GP nerve activity, and abolishes the electrophysiological response seen during apnea.

A critical role of a neurosensory reflex in apnea-induced AF is suggested and could potentially be therapeutically targeted.

Supplementary Material

Refer to Web version on PubMed Central for supplementary material.

Acknowledgments:

The authors would like to thank Holly Zapalac, Daryl Schulz, Caroline White, Courtney Vallien and Maga Sanchez for their technical assistance.

Sources of Funding: Supported by NIH/NHLBI R01 HL115003 (United States), the Charles Burnett III and the Lois and Carl Davis Centennial Chair endowments (Houston, Texas, United States).

References:

1. Ghias M, Scherlag BJ, Lu Z, Niu G, Moers A, Jackman WM, Lazzara R, Po SS. The role of ganglionated plexi in apnea-related atrial fibrillation. J Am Coll Cardiol. 2009;54:2075–83. [PubMed: 19926016]
2. Gao M, Zhang L, Scherlag BJ, Huang B, Stavrakis S, Hou YM, Hou Y, Po SS. Low-level vagosympathetic trunk stimulation inhibits atrial fibrillation in a rabbit model of obstructive sleep apnea. Heart Rhythm. 2015;12:818–24. [PubMed: 25533582]
3. Linz D, Schotten U, Neuberger HR, Bohm M, Wirth K. Negative tracheal pressure during obstructive respiratory events promotes atrial fibrillation by vagal activation. Heart Rhythm. 2011;8:1436–43. [PubMed: 21457790]

4. Ardell J. Structure and function of mammalian intrinsic cardiac neurons In: Armour JAA, L J, ed Neurocardiology New York: Oxford University Press 1994:95–114.
5. Wake E, Brack K. Characterization of the intrinsic cardiac nervous system. Auton Neurosci. 2016;199:3–16. [PubMed: 27568996]
6. Urban L, Papka RE. Origin of small primary afferent substance P-immunoreactive nerve fibers in the guinea-pig heart. J Auton Nerv Syst. 1985;12:321–31. [PubMed: 2582024]
7. Dalsgaard CJ, Franco-Cereceda A, Saria A, Lundberg JM, Theodorsson-Norheim E, Hokfelt T. Distribution and origin of substance P- and neuropeptide Y-immunoreactive nerves in the guinea-pig heart. Cell Tissue Res. 1986;243:477–85. [PubMed: 2420458]
8. Szallasi A, Blumberg PM. Resiniferatoxin, a phorbol-related diterpene, acts as an ultrapotent analog of capsaicin, the irritant constituent in red pepper. Neuroscience. 1989;30:515–20. [PubMed: 2747924]
9. Walpole CS, Bevan S, Bloomfield G, Breckenridge R, James IF, Ritchie T, Szallasi A, Winter J, Wrigglesworth R. Similarities and differences in the structure-activity relationships of capsaicin and resiniferatoxin analogues. J Med Chem. 1996;39:2939–52. [PubMed: 8709128]
10. Caterina MJ, Schumacher MA, Tominaga M, Rosen TA, Levine JD, Julius D. The capsaicin receptor: a heat-activated ion channel in the pain pathway. Nature. 1997;389:816–24. [PubMed: 9349813]
11. Szallasi A, Blumberg PM. Vanilloid receptor loss in rat sensory ganglia associated with long term desensitization to resiniferatoxin. Neurosci Lett. 1992;140:51–4. [PubMed: 1407700]
12. Olah Z, Szabo T, Karai L, Hough C, Fields RD, Caudle RM, Blumberg PM, Iadarola MJ. Ligand-induced dynamic membrane changes and cell deletion conferred by vanilloid receptor 1. J Biol Chem. 2001;276:11021–30. [PubMed: 11124944]
13. Zahner MR, Li DP, Chen SR, Pan HL. Cardiac vanilloid receptor 1-expressing afferent nerves and their role in the cardiogenic sympathetic reflex in rats. J Physiol. 2003;551:515–23. [PubMed: 12829722]
14. Wang HJ, Wang W, Cornish KG, Rozanski GJ, Zucker IH. Cardiac sympathetic afferent denervation attenuates cardiac remodeling and improves cardiovascular dysfunction in rats with heart failure. Hypertension. 2014;64:745–55. [PubMed: 24980663]
15. Robinson EA, Rhee KS, Doytchinova A, Kumar M, Shelton R, Jiang Z, Kamp NJ, Adams D, Wagner D, Shen C, Chen LS, Everett TH, Fishbein MC, Lin SF, Chen PS. Estimating sympathetic tone by recording subcutaneous nerve activity in ambulatory dogs. J Cardiovasc Electrophysiol. 2015;26:70–8. [PubMed: 25091691]
16. Foley JO, DuBois FS. Quantitative studies of the vagus nerve in the cat. I. The ratio of sensory to motor fibers. J Comp Neurol. 1937;67:49–67.
17. Chang RB, Strochlic DE, Williams EK, Umans BD, Liberles SD. Vagal Sensory Neuron Subtypes that Differentially Control Breathing. Cell. 2015;161:622–633. [PubMed: 25892222]
18. Onkka P, Maskoun W, Rhee KS, Hellyer J, Patel J, Tan J, Chen LS, Vinters HV, Fishbein MC, Chen PS. Sympathetic nerve fibers and ganglia in canine cervical vagus nerves: localization and quantitation. Heart Rhythm. 2013;10:585–91. [PubMed: 23246597]
19. Wickramasinghe SR, Patel VV. Local innervation and atrial fibrillation. Circulation. 2013;128:1566–75. [PubMed: 24081952]
20. Adams DJCJ Electrophysiological properties of intrinsic cardiac neurons In: Armour JAA, L. J, ed. Basic and clinical neurocardiology New York: Oxford University Press; 2004: 1–60.
21. Konishi S, Otsuka M. Blockade of slow excitatory post-synaptic potential by substance P antagonists in guinea-pig sympathetic ganglia. J Physiol. 1985;361:115–30. [PubMed: 2580973]
22. Hardwick JC, Mawe GM, Parsons RL. Evidence for afferent fiber innervation of parasympathetic neurons of the guinea-pig cardiac ganglion. J Auton Nerv Syst. 1995;53:166–74. [PubMed: 7560753]
23. Cervero F Sensory innervation of the viscera: peripheral basis of visceral pain. Physiol Rev. 1994;74:95–138. [PubMed: 8295936]
24. Downar E, Janse MJ, Durrer D. The effect of acute coronary artery occlusion on subepicardial transmembrane potentials in the intact porcine heart. Circulation. 1977;56:217–24. [PubMed: 872313]

25. Yoshie K, Rajendran PS, Massoud L, Kwon O, Tadimeti V, Salavatian S, Ardell JL, Shivkumar K, Ajijola OA. Cardiac vanilloid receptor-1 afferent depletion enhances stellate ganglion neuronal activity and efferent sympathetic response to cardiac stress. Am J Physiol Heart Circ Physiol. 2018;314:H954–H966. [PubMed: 29351450]

26. May AM, Van Wagoner DR, Mehra R. OSA and Cardiac Arrhythmogenesis: Mechanistic Insights. Chest. 2017;151:225–241. [PubMed: 27693594]

27. Iwasaki YK, Kato T, Xiong F, Shi YF, Naud P, Maguy A, Mizuno K, Tardif JC, Comtois P, Nattel S. Atrial fibrillation promotion with long-term repetitive obstructive sleep apnea in a rat model. J Am Coll Cardiol. 2014;64:2013–23. [PubMed: 25440097]

WHAT IS KNOWN?

- The precise mechanisms for the association between obstructive sleep apnea and atrial fibrillation (AF) are unclear, but a prominent role of the autonomic nervous system is suspected.
- Radiofrequency ablation of the intrinsic cardiac autonomic nervous system (intrinsic cardiac ganglionated plexi) inhibits apnea-induced atrial fibrillation.

WHAT THE STUDY ADDS?

- Apnea induces a complex response of the autonomic nervous system including intrinsic cardiac ganglionated plexi (GP) firing, phasic vagal bursts coinciding with heart rate and blood pressure oscillations, and tonic stellate ganglion (SG) firing that lead to atrial effective refractory period (ERP) shortening and increased AF inducibility.
- Chemical ablation of GP sensory neurons with resiniferatoxin, a neurotoxic transient receptor potential vanilloid 1 (TRPV1) agonist, decreases GP and SG activity, abolishes apnea's electrophysiological response, and inhibits AF induction.
- GP sensory neurons play a role in apnea-induced AF and could potentially be therapeutically targeted.

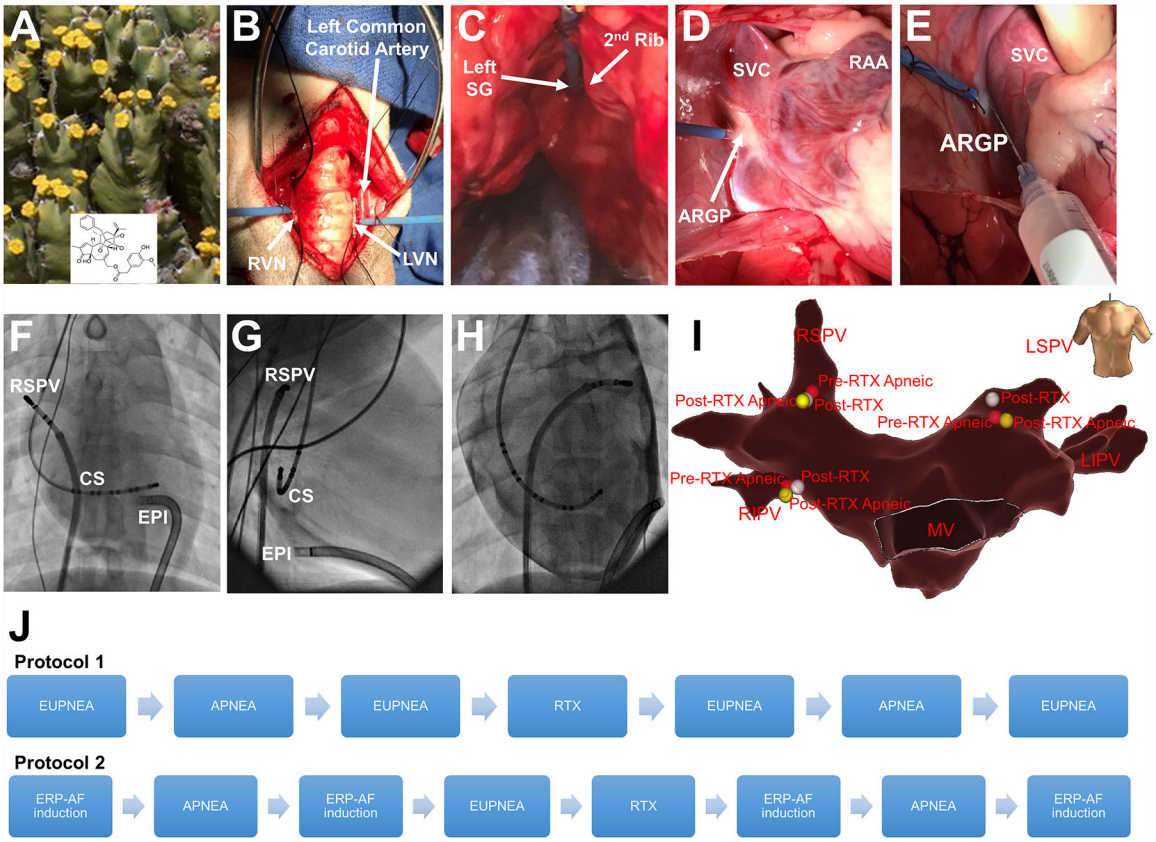

Figure 1.

Overview of protocols 1 and 2. *Euphorbia resinifera*, a cactus-like plant from where RTX is obtained (A). Representative examples of cervical RVN and LVN (B), left SG (C) and anterior right GP (D) with recording electrodes. Location of RTX injection in ARGP (E). Anteroposterior fluoroscopic view showing the sheath in the epicardium (EPI), the decapolar catheter in the CS and the deflectable catheter placed in the RSPV (F). Right anterior oblique view (G). Left anterior oblique view after epicardial contrast (H). Electroanatomical 3D reconstruction (anteroposterior view) of the left atrium displaying the three locations points studied, RSPV (location 1), LSPV (location 2) and RIPV (location 3) (I). Schematic representation of protocols 1 and 2 (J). ARGP, anterior right ganglionated plexi; CS, coronary sinus; GP, ganglionated plexi; LSPV, left superior pulmonary vein; LVN, left vagal nerve; RAA, right atrial appendage; RIPV, right inferior pulmonary vein; RSVP, right superior pulmonary vein; RTX, resiniferatoxin; RVN, right vagal nerve; SG, stellate ganglion; SVC, superior vena cava.

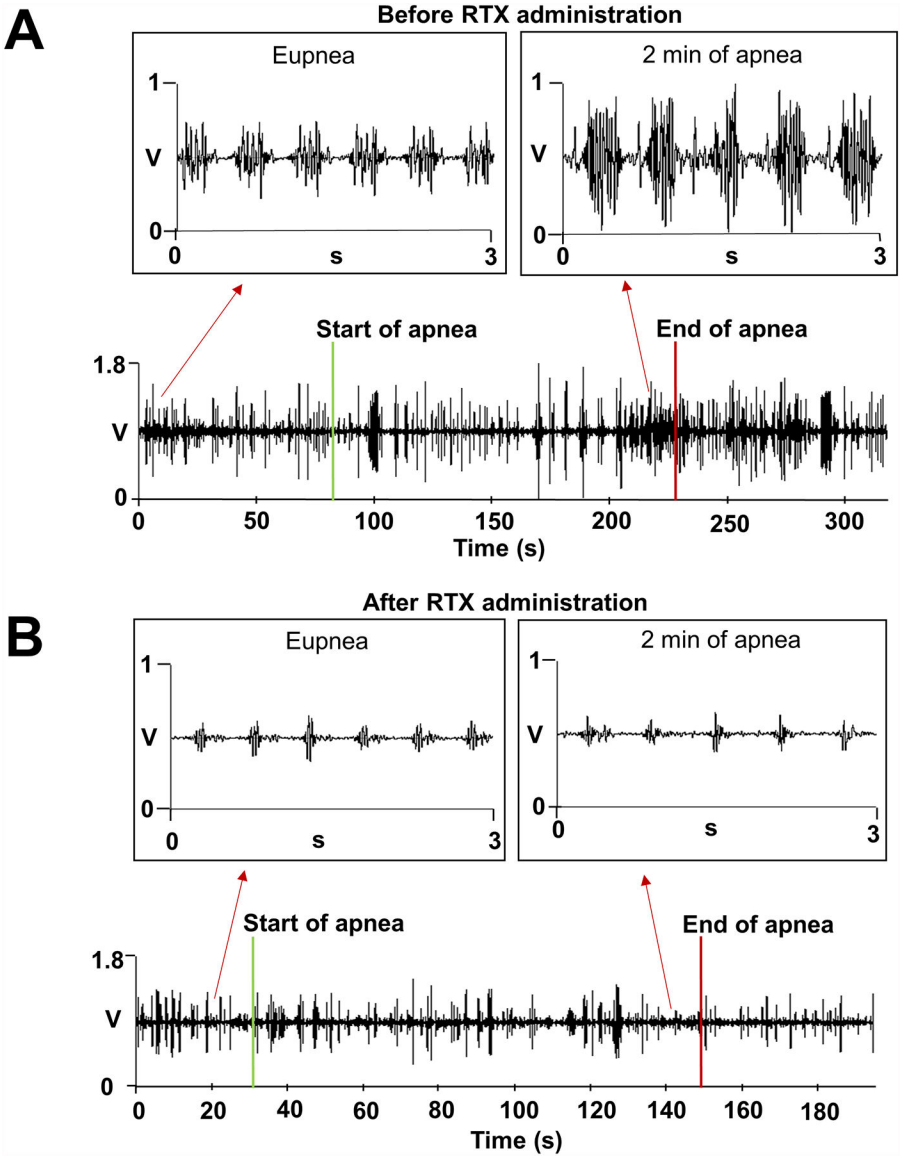

Figure 2.

Anterior right GP activity during apnea before and after local RTX injection. A. An example of anterior right GP activity during apnea before RTX injection. Upon apnea initiation no discernible changes in GP activity were seen, but as apnea progressed and SaO2 declined, GP activity increased, with the highest increase in activity noted at 2 min of apnea with a SaO2 of 85%. B. An example of anterior right GP activity during apnea after RTX injection. GP recordings after RTX showed no increased activity during apnea. SaO2, oxygen saturation; other abbreviations as in Figure 1.

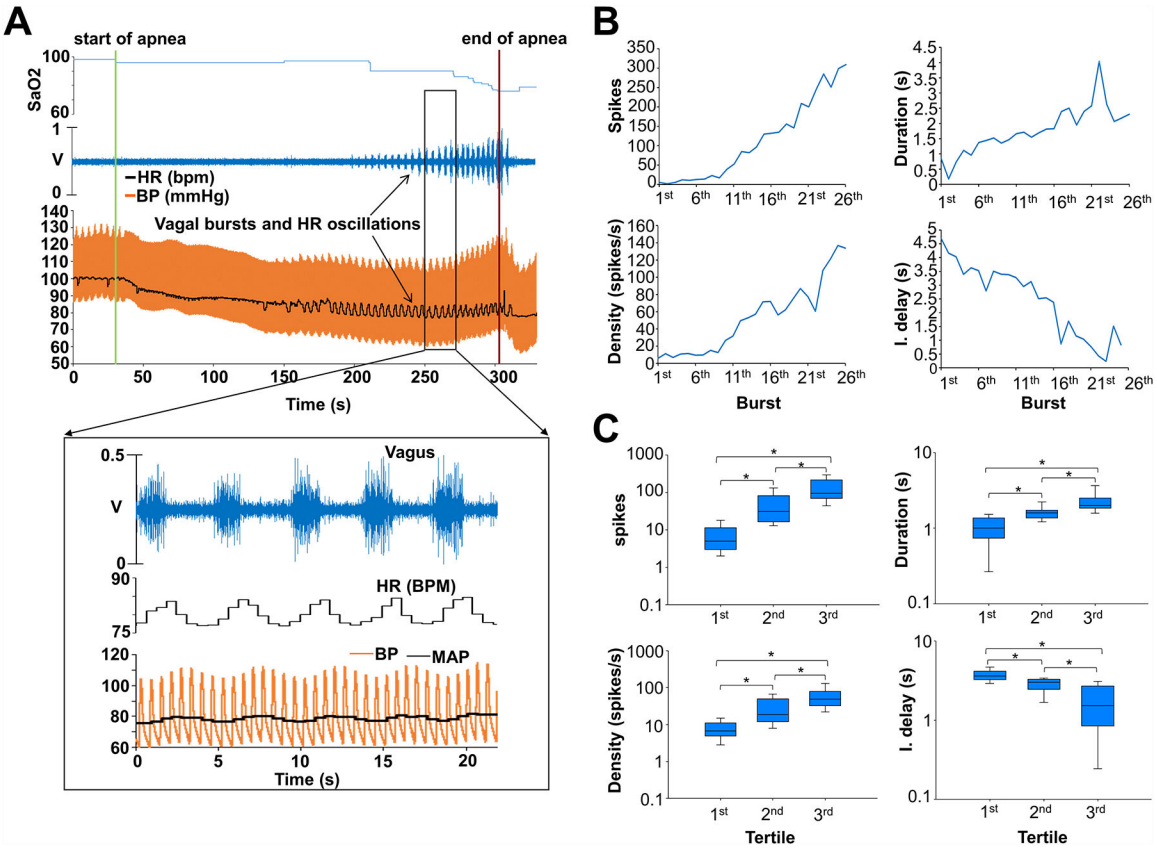

Figure 3.

Vagal activity during apnea before RTX injection. A and B. Example of vagal nerve activity during apnea before RTX. Initially no detectable changes were seen in the vagal activity. However, as SaO2 declined changes in the activity occurred, in the form of crescendo phasic bursts of discharges that coincided with HR and BP oscillations. Vagal bursts started after 2 minutes and 34 seconds of apnea and with a SaO2 of 97%. The number of spikes, the duration and the density (spikes/duration) of each burst progressively increased as apnea continued. The time interval between bursts (interburst delay) decreased. C. Vagal burst activity during apnea divided in tertiles. A progressive and significant increase in vagal bursts during apnea was observed (from burst onset to apnea end, all tertiles $p<0.001$). Data expressed as median and interquartile range. *, Statistical significance set at $p<0.017$. BP, blood pressure; HR, heart rate; other abbreviations as in Figure 1 and 2.

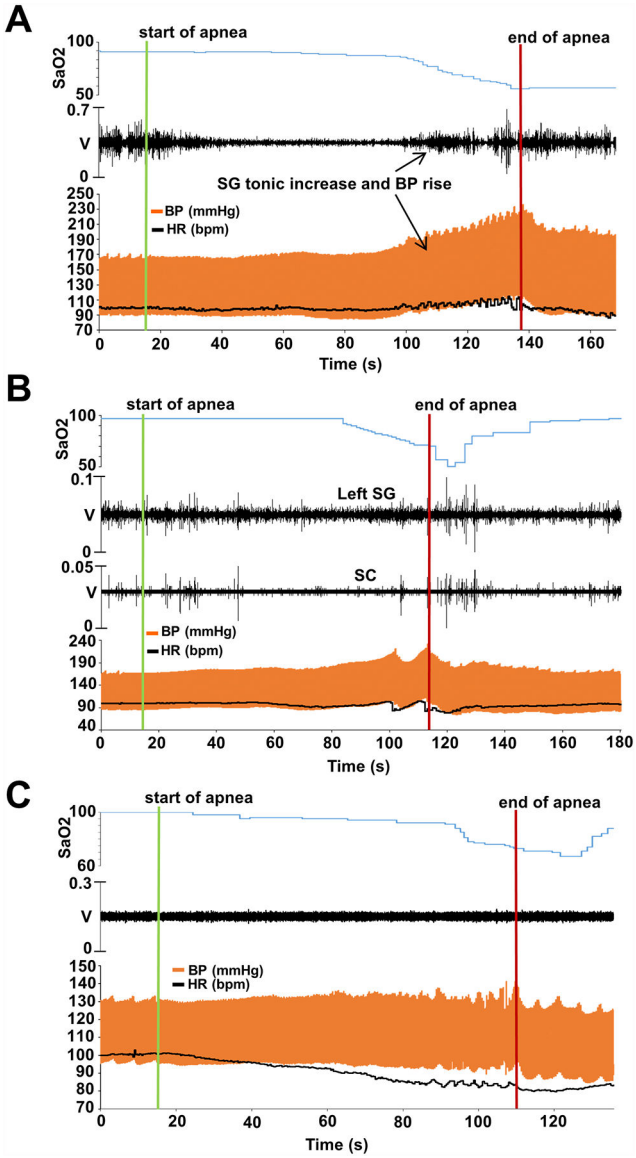

Figure 4.

Sympathetic activity during apnea before and after local RTX injection. A. An example of SG activity during apnea before RTX injection. Initially a decrease in SG amplitude was seen, but as apnea continued and SaO2 declined, there was a progressive increase in SG recording amplitude that coincided with HR and BP increases. SG activity began to increase after 1 min and 21 seconds of apnea and with a SaO2 of 93%. B. SG and SC activity during apnea. We observed that SC nerve activity closely matched that of the SG. C. An example of SG activity during apnea after RTX injection. The increased SG activity, previously observed, which had correlated with the HR and BP increase was abolished after RTX. SC, subcutaneous; other abbreviations as in Figure 1, 2 and 3.

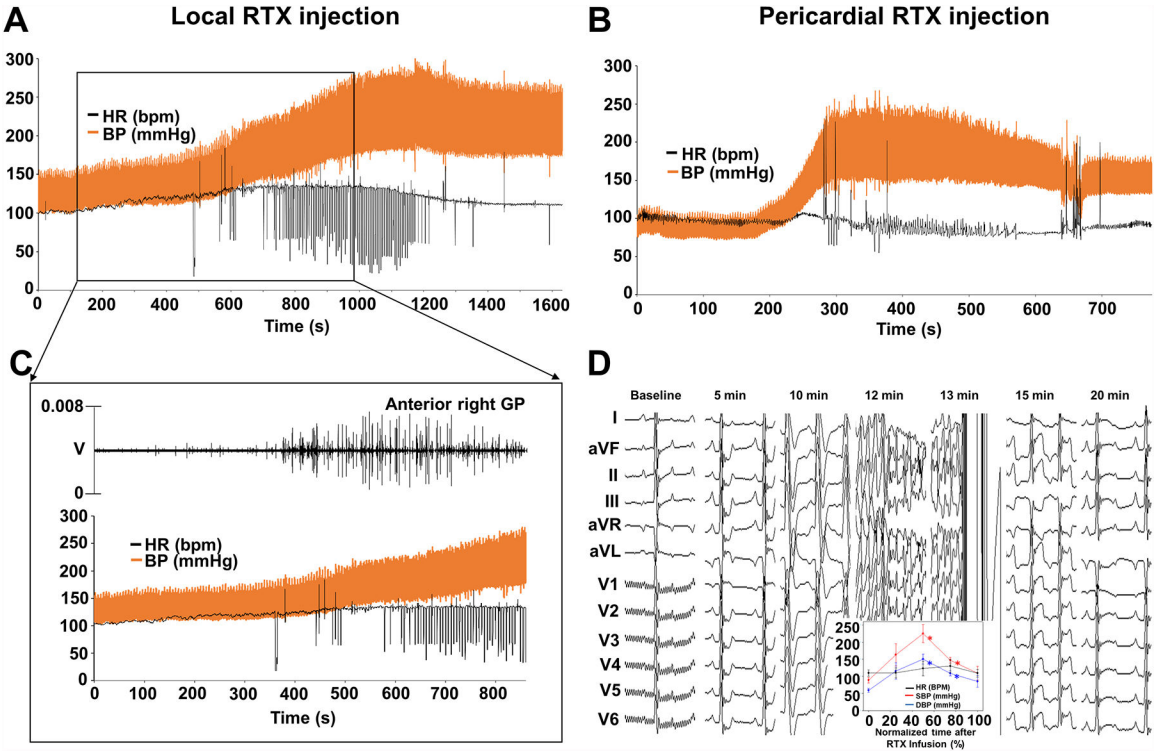

Figure 5.

Acute GP-RTX-induced changes. Both routes of injection led to vascular lability with dramatic increases in systolic BP within less than 20 minutes of infusion in all animals. A. An example of immediate RTX-induced changes caused by local-RTX injection. HR, SBP and DBP increased within 3 minutes and 20 seconds of injection. B. An example of immediate RTX-induced changes caused by intrapericardial-RTX injection. HR, SBP and DBP increased within 3 minutes of injection. C. Increases in BP and HR were paralleled by increases in ARGP activity. D. Sequential electrocardiographic changes recorded. ST-segment changes and QRS widening. DBP, diastolic blood pressure; SBP, systolic blood pressure; other abbreviations as in Figures 1, 2 and 3.

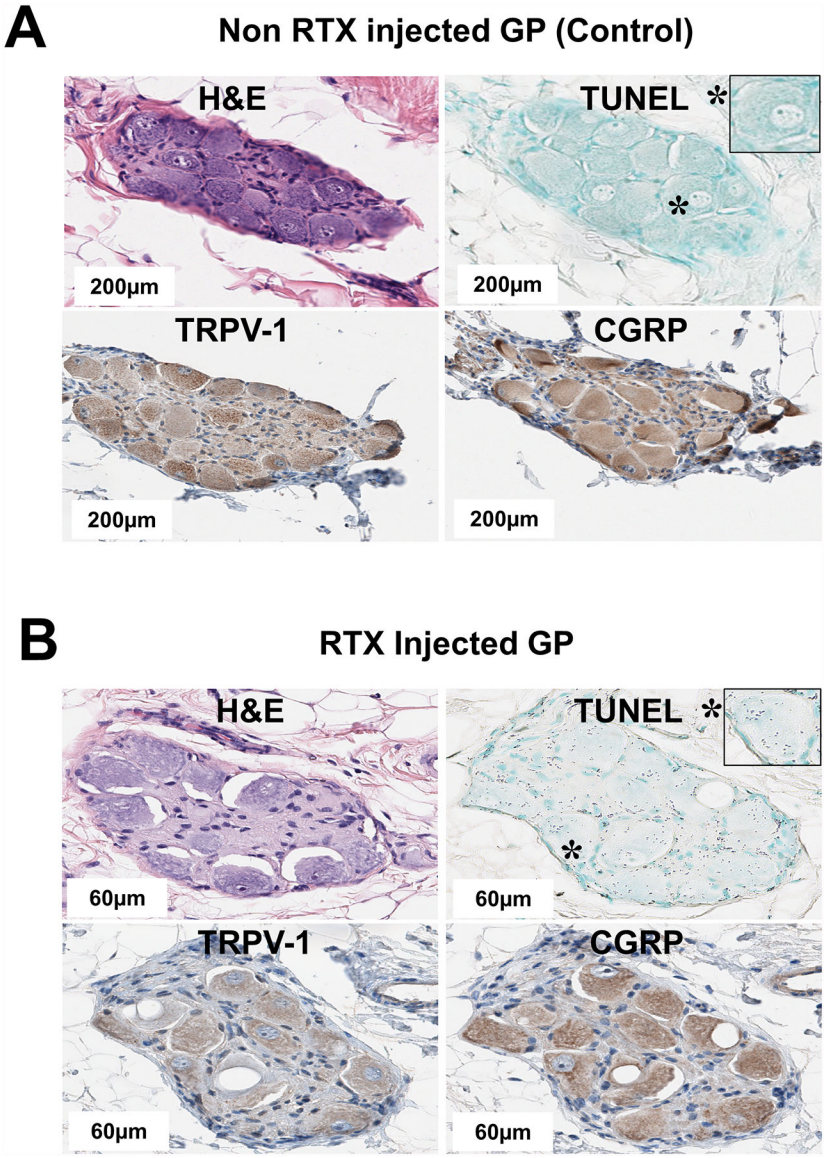

Figure 6.

Histopathology studies of the GP. A. H&E, TUNEL, TRPV-1 and CGRP staining of non RTX injected GP (control). Individual cells within the ganglion were positive for sensory neuronal markers TRPV1 and CGRP, and were not apoptotic (TUNEL-negative). B. H&E, TUNEL, TRPV1 and CGRP staining of RTX injected GP. Some individual ganglion cells morphologically displayed cytoplasmic micro and macro vacuolization. Cells bluntly stained for TRPV1 and CGRP and were apoptotic (TUNEL-positive). CGRP, calcitonin gene-related peptide; H&E, hematoxylin and eosin; TRPV1, transient receptor potential vanilloid 1; TUNEL, terminal deoxynucleotidyl transferase dUTP-mediated nick end labelling; other abbreviations as in Figure 1.

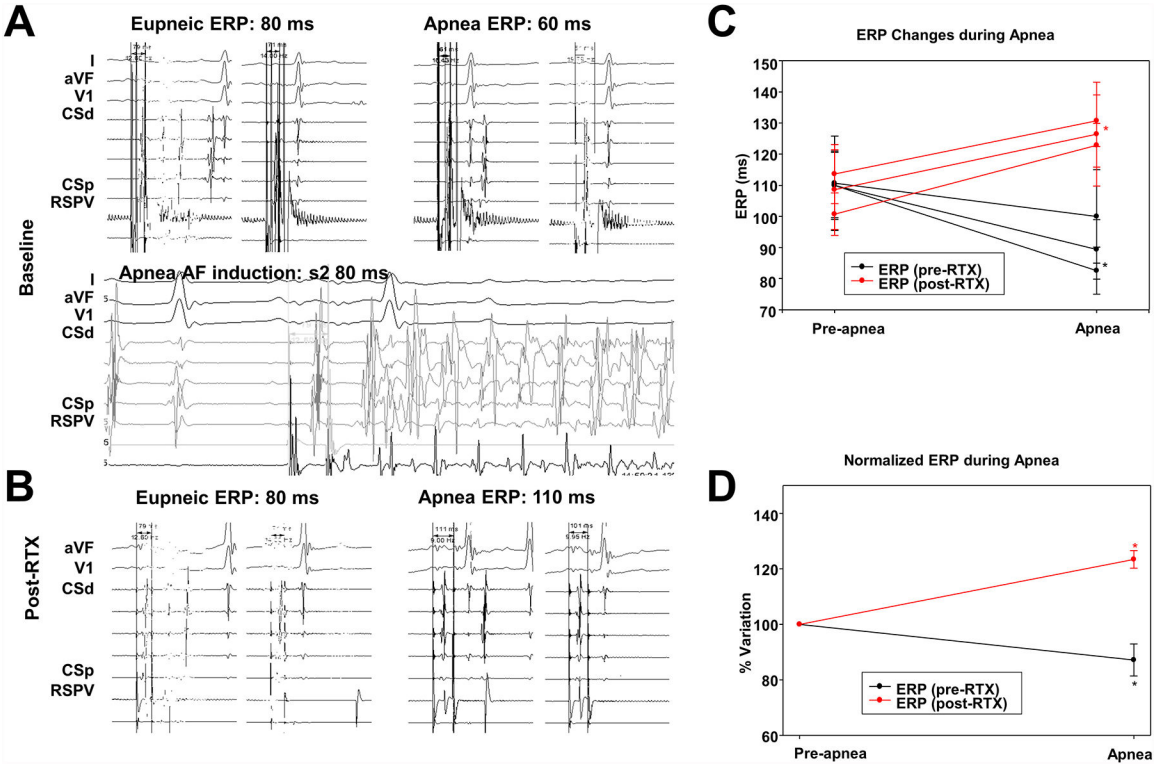

Figure 7.

Electrophysiological response to apnea before and after RTX injection. A. An example of ERP changes during apnea before RTX injection. Apnea led to ERP decrease, from a baseline of 400/80 ms to 400/60 ms, and AF induction with left atrial single extrastimulation. B. An example of ERP changes during apnea after RTX injection. The ERP increased during apnea after RTX injection, from a baseline of 400/80 ms to 400/110 ms. C. Absolute atrial ERP changes noted in location 1 (RSPV), location 2 (LSPV) and location 3 (RIPV) during apneic episodes before (black line) and after (red line) RTX. D. Normalized averaged atrial ERP variation during apneic episodes before (black line) and after (red line) RTX. Data expressed as mean ± SD. *, P<0.05, significance level set at p<0.025. AF, atrial fibrillation; ERP, atrial effective refractory period; other abbreviations as in Figure 1.